Magnetostatic Field Analysis by Method of Images

Beca

www.beca.com

Presented by: Michael Owen

Beca, PO Box 6345, Auckland 1141, New Zealand,
michael.owen@beca.com

Abstract

The Method of Images is applied to a filamentary current flowing in a void parallel to the four sides of an infinitely permeable surface. The magnetic vector potential and magnetic flux density are calculated in the void region. The calculation is verified by using both direct summation of the fields due to the source and images, and also by use of a series summation in terms of Weierstraß's sigma and zeta functions.

Keywords: Method of Images, Weierstraß, Magnetostatic.

1. Introduction

Whilst magnetostatic field analysis is commonly performed on computers using the Finite Element Method, the student is left without a full appreciation of the physics involved in the development of that field. This paper builds on previous analytical work with the aim of providing a greater insight into the evolution of a magnetostatic field.

In a previous publication Hicks [1] attempted to solve the two-dimensional electrostatic field problem of a charged wire within the void of a rectangular tube made from conducting material. The solution, which is in terms of Jacobian elliptic functions, is however flawed due to an algebraic error occurring during the separation of two squares. Also, for the same shape, Hague [2] attempted to solve the conjugate two-dimensional magnetostatic problem. The source consisted of a filamentary current flowing in a void parallel to four of its sides. The sides were postulated to be made of a material with infinite permeability. The material and filament extended to infinity in both directions along one axis. The field solution for the void in the plane perpendicular to that axis was given as a series of circular functions, but lacked an overall expression for its sum. Hague did not tabulate or plot results for his proposed formulation. The author has now reconsidered the formulations and consequently derived an alternative solution in terms of Weierstraß's zeta and sigma functions. The analysis presented is based upon the Method of Images [3] and develops the subject using magnetostatic equations.

2. Conceptual Model

The geometry of the model arises as a consequence of the Method of Images and follows the optical pattern. The inner sides of the tube representing the material interface behave as mirrors. An infinite number of filament images, of equivalent amplitude and direction to the source, are thus arranged symmetrically about the source location. Fig. 1 depicts the arrangement in the X–Y plane where:

W, L are the width and height of the tube respectively.
s, h are the respective x, y coordinates of the filament.
$\boldsymbol{\alpha}$ are image series based upon the first image points.
$\boldsymbol{\beta}$ is the image series based upon the source point.

Shown in parentheses alongside each image are the image multiples that occur at each point.

The resultant magnetostatic field in the tube is due to the sum of the fields of the source plus all its images, with the intervening space between source and images treated wholly as a homogeneous void. In this model therefore, the material at the surface has been replaced by the system of the images set in an infinite and continuous void.

3. Magnetostatic Formulation

From the experimental observations of Biot and Savart, using polar co-ordinates with unit vector $\boldsymbol{\alpha}$, and ignoring constants of proportionality:

$$\boldsymbol{B} = \frac{I}{\rho_Z} .\alpha_\varphi \qquad (1)$$

where $\boldsymbol{B}$ is the magnetic flux density at a radius $\boldsymbol{\rho}$ perpendicular to the filamentary current I.

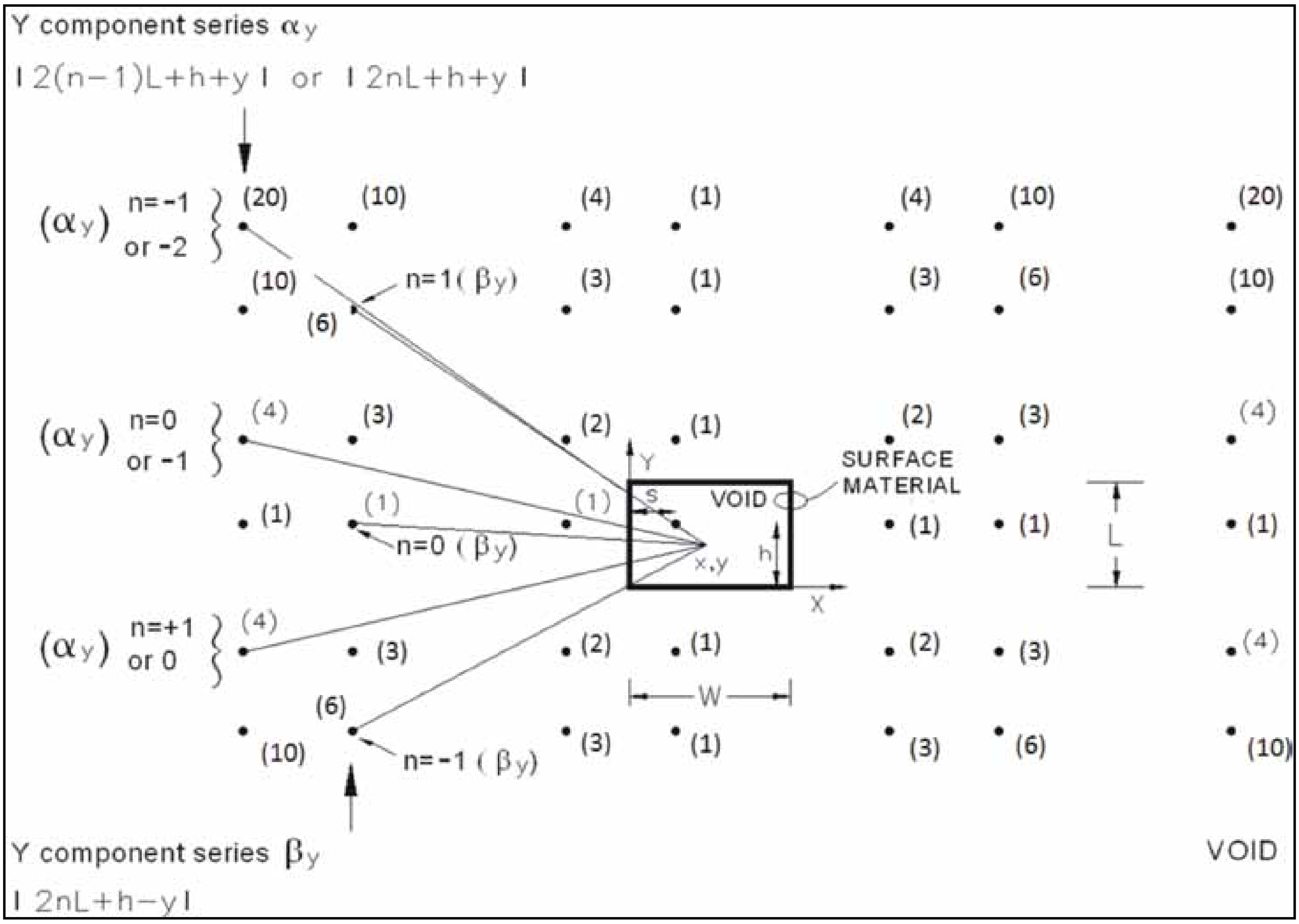

Figure 1: System Geometry in the X-Y plane

From the definition of the magnetic vector potential A:

$$\boldsymbol{B} = \nabla \times \boldsymbol{A} \quad (2)$$

And also due to the singular direction of the current, at the point (x,y):

$$\boldsymbol{A} = \boldsymbol{A}_Z\, \boldsymbol{\alpha}_Z \quad (3)$$

then for a unit quantity of current:

$$-\frac{\partial A_Z}{\partial \rho}\boldsymbol{a}_\varphi = \frac{1}{\rho_Z}\,.\,\boldsymbol{a}_\varphi \quad (4)$$

and:

$$\boldsymbol{A}_Z = \boldsymbol{C} - \ln(\rho_Z) \quad (5)$$

In Fig. 1 the X and Y components of the distance between the images and a point (x,y) within the rectangle are given by:

X component $|2(m-1)W + s + x|$ (6)

for series $\boldsymbol{\alpha}_x$ or

$|2mW + s + x|$ (7)

and for series βx $|2mW + s - x|$ (8)

Y component $|2(n-1)L + h + y|$ (9)

or

for series $\boldsymbol{\alpha}_y$ $|2nL + h + y|$ (10)

and

for series β_y $|2nL + h - y|$ (11)

For $-\infty \le m, n \le \infty$

The magnetic vector potential A_z at the point (x,y) due to the various series of images is therefore:

$A_{z,\beta\beta} = C_{\beta\beta} - \Sigma' \ln[(2mW - x + s)^2 + (2nL - y + h)^2]^{1/2}$ (12)

$A_{z,\beta\beta} = C_{\alpha\beta} - \Sigma' \ln[(2mW + x + s)^2 + (2nL - y + h)^2]^{1/2}$ (13)

{or $A_{z,\alpha\beta} = C_{\alpha\beta} - \Sigma' \ln[(2mW + x + (s - 2W))^2 + (2nL - y + h)^2]^{1/2}$ } (14)

$$A_{z,\beta\alpha} = C_{\beta\alpha} - \Sigma' \ln [(2mW - x + s)^2 + (2nL + y + h)^2]^{1/2} \quad (15)$$

$$\{\text{or } A_{z,\beta\alpha} = C_{\beta\alpha} - \Sigma' \ln [(2mW - x + s)^2 + (2nL + y + (h - 2L))^2]^{1/2} \} \quad (16)$$

$$A_{z,\alpha\alpha} = C_{\alpha\alpha} - \Sigma' \ln [(2mW + x + s)^2 + (2nL + y + h)^2]^{1/2} \quad (17)$$

$$\{\text{or } A_{z,\alpha\alpha} = C_{\alpha\alpha} - \Sigma' \ln [(2mW + x + (s - 2W))^2 + (2nL + y + h)^2]^{1/2} \} \quad (18)$$

$$\{\text{or } A_{z,\alpha\alpha} = C_{\alpha\alpha} - \Sigma' \ln [(2mW + x + s)^2 + (2nL + y + (h - 2L))^2]^{1/2} \quad (19)$$

$$\{\text{or } A_{z,\alpha\alpha} = C_{\alpha\alpha} - \Sigma' \ln [(2mW + x + (s - 2W))^2 + (2nL + y + (h - 2L))^2]^{1/2} \} \quad (20)$$

where the summation takes the values of m and n over the complete range of integers with the exception of the paired zero points $m = n = 0$. This is indicated by the prime symbol following the summation sign. The magnetic vector potential due to the paired zero points is treated separately and identified as $A_{z,00}$.

In the case of the (α_x, α_y) series, four alternatives are shown. The method takes one quarter of the sum of these four series to ensure the solution remains symmetrical about the source entity. The same principle is applied to other contributions of the α and β series. For the paired zero terms which occur at the source and the surrounding eight images, the additional contribution is accounted for in the $A_{z,00}$ term.

Expanding the summation term of the magnetic vector potential for the (β_x, β_y) series in terms of infinite products results in:

$$A_{z,\beta\beta} = -0.5 \ \Re \ [\ln \Pi' (1 - \boldsymbol{u}_{\beta\beta} / \Omega_{n,m}) + \ln \Pi' (1 - \tilde{\boldsymbol{u}}_{\beta\beta} / \tilde{\Omega}_{n,m})] \quad (21)$$

where the product takes the value of m and n over the complete range of integers with the exception of the paired zero points $m = n = 0$, and:

$$i = \sqrt{-1}$$
$$\boldsymbol{u}_{\beta\beta} = (x - s) + i\,(y - h)$$
$$\tilde{\boldsymbol{u}}_{\beta\beta} = (y - h) + i\,(x - s)$$
$$\Omega_{n,m} = (2mW + i\,2nL)$$
$$\tilde{\Omega}_{n,m} = (2nL + i\,2mW)$$
$$C_{\beta\beta} = 0.5 \ln \Pi' (i\,\Omega_{n,m}\,\tilde{\Omega}_{n,m})$$

Since Weierstraß's sigma function [4] may be expressed as:

$$\sigma(u, \Omega) = \Pi' [(1 - u / \Omega_{n,m}) \exp\{(u / \Omega_{n,m}) + (u^2 / 2\Omega_{n,m}^{\ 2})\}] \quad (22)$$

subject to the condition:

$\lim \{ \sigma(u) / u\} = 1, u \to 0$

then:

$$\ln \Pi' (1 - u / \Omega_{n,m}) = \ln (\sigma(u, \Omega) / u) - u \Sigma' (1 / \Omega_{n,m}) - u^2 \Sigma' (1 / 2\Omega_{n,m}^{\ 2}) \quad (23)$$

therefore:

$$A_{z,\beta\beta} = -0.5 \ \Re \ [\ln (\sigma (u_{\beta\beta}, \Omega) / u_{\beta\beta}) - u_{\beta\beta} \Sigma'(1 / \Omega_{n,m}) - u_{\beta\beta}^{\ 2} \Sigma' (1 / 2\Omega_{n,m}^{\ 2}) + \ln (\sigma(\tilde{u}_{\beta\beta}, \tilde{\Omega}) / \tilde{u}_{\beta\beta}) - \tilde{u}_{\beta\beta} \Sigma' (1 / \tilde{\Omega}_{n,m}) - \tilde{u}_{\beta\beta}^{\ 2} \Sigma' (1 / 2\tilde{\Omega}_{n,m}^{\ 2})] \quad (24)$$

The other series terms may be expressed in similar forms. The final magnetic vector potential is thus:

$$A_z = A_{z,00} + \Sigma A_{z,\ (\text{series terms})} \quad (25)$$

The magnetic flux density is derived by applying Eq. (2) in its Cartesian form to Eq. (12) through to Eq. (20). Then, as $\boldsymbol{B}$ has only x and y components:

$$\boldsymbol{B}_{\alpha\alpha} = \nabla \times \boldsymbol{A}_{\alpha\alpha} = - \Sigma' (1 / (\tilde{u}_{\alpha\alpha} - \tilde{\Omega}_{n,m})) \quad (26)$$

Also using the following expression for Weierstraß's zeta function [4]:

$$\zeta(u, \Omega) = 1/u + \Sigma' (1 / (u - \Omega_{n,m})) + \Sigma' (1 / \Omega_{n,m}) + u \Sigma' (1 / \Omega_{n,m}^{\ 2}) \quad (27)$$

then:

$$\boldsymbol{B}_{\alpha\alpha} = - [\zeta(\tilde{u}_{\alpha\alpha}, \tilde{\Omega}) - 1/\tilde{u}_{\alpha\alpha} - \Sigma' (1 / \tilde{\Omega}_{n,m}) - \tilde{u} \Sigma' (1 / \tilde{\Omega}_{n,m}^{\ 2}))] \quad (28)$$

and finally:

$$\boldsymbol{B} = \nabla \times \boldsymbol{A}_{\alpha\alpha} + \Sigma \boldsymbol{B}_{(\text{series terms})} \quad (29)$$

$$\text{with:} \quad |\boldsymbol{B}| = \sqrt{\left(\frac{\partial A_z}{\partial x}\right)^2 + \left(\frac{\partial A_z}{\partial y}\right)^2} \quad (30)$$

In order to assure symmetry in the result the summation takes account of the multiples of each image, in a manner similar to the technique used for the magnetic vector potential.

An application of the method is shown in Fig. 2. Contour plots show the magnetic vector potential and magnetic flux density.

The graphs have been extended to show a number of images outside the tube region in order to fully demonstrate the nature of the fields.

To verify the results, both the Weierstraß function and direct programming of the series were implemented. In the direct programming case, a reflection depth of five was found sufficient to give a comparable result.

4. Conclusion

An analytical approach has been successfully applied to solve the magnetostatic field problem for a filamentary current flowing in a void parallel to four sides of a tube, postulated to be made of a material with infinite permeability. The Method of Images provides an insight into the development of the field via a set of reflected traveling waves from apparent sources that correspond to the images used in the analysis.

Acknowledgment

The author acknowledges the support of Beca Carter Hollings & Ferner for the presentation of this paper. The author also acknowledges Fay Yuen for his assistance with the calculations.

References

1. Hicks, W.M. (1878), ‘On velocity and electric potentials between parallel planes’, Quarterly J. of Pure and Appl. Math, XV, 274-315.
2. Hague, B. (1926), ‘The electromagnetic forces on conductors near iron’, World Power, (V) XXVIII, pp. 205-211.
3. Kelvin, Lord. (1848), (see Thomson, W. 1848, Reprint of paper on electrostatics and magnetism, 2nd edn, pp. 52-85. Macmillan, London).
4. Whittaker, E.T. & Watson, G.N. (1927), A course of modern analysis, Cambridge University Press.

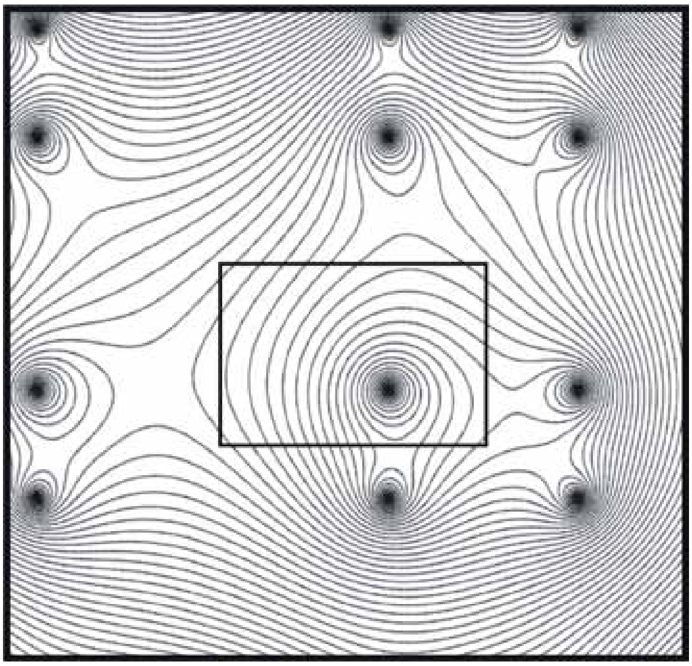

Figure 2a

Magnetic Vector Potential A
Rectangular tube, offset source, aspect ratio = 3:2

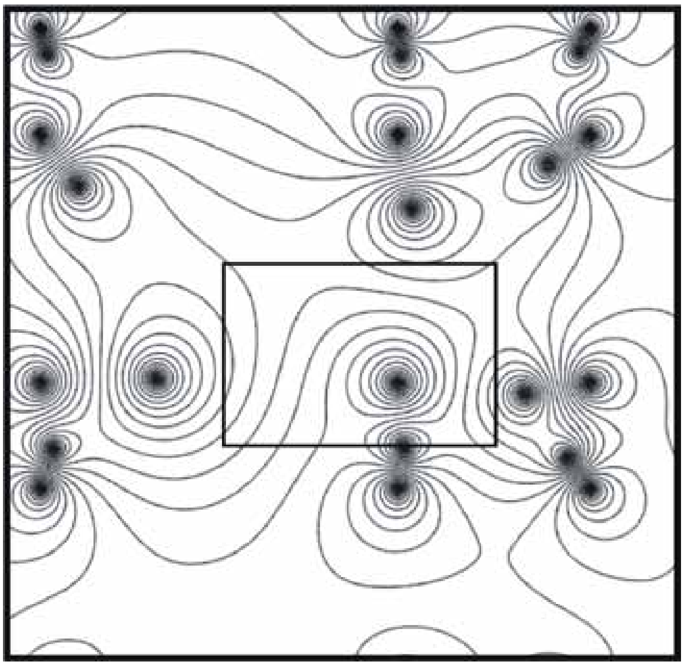

Figure 2b

Magnetic Flux Density B
Rectangular tube, offset source, aspect ratio = 3:2